Vol. 638: 51–63, 2020
https://doi.org/10.3354/meps13250

MARINE ECOLOGY PROGRESS SERIES
Mar Ecol Prog Ser

Published March 19

Vortical feeding currents in nauplii of the calanoid copepod *Eucalanus pileatus*

Houshuo Jiang[1,*], Gustav-Adolf Paffenhöfer[2]

[1]Department of Applied Ocean Physics and Engineering, Woods Hole Oceanographic Institution, Woods Hole, Massachusetts 02543, USA

[2]Skidaway Institute of Oceanography, 10 Ocean Science Circle, Savannah, Georgia 31411, USA

ABSTRACT: The goal of this study was to quantify feeding-current generation processes in mid to late nauplii and early copepodites of the calanoid copepod *Eucalanus pileatus*. Using a high-speed microscale imaging system (HSMIS) to conduct both microvideography and micro-particle image velocimetry (μPIV), free-swimming nauplii of *E. pileatus* were shown to use a novel 'double draw-and-cut' continuous appendage beat pattern, which is nonreciprocal, to generate a vortical feeding current at a Reynolds number of ~0.8. The feeding current consists of a core flow towards the ventral surface and 2 laterally flanking viscous vortices reinforcing the core flow. This feeding current is spatially limited with an r^{-3} decay, potentially reducing predation by rheotactic predators. The feeding current displaces water at ~1.0×10^6 naupliar body volumes per day towards the mouthpart zone. This would result in a clearance rate providing sufficient food at a relatively high environmental food concentration. HSMIS videos revealed that *E. pileatus* nauplii combine their feeding current and swimming motion to displace algae towards their mouth for capture, and can react to an incoming alga at a 300–500 μm distance away from the nearest naupliar setae, indicating remote detection presumably via chemoreception. The r^{-3}-decay naupliar feeding current is suggested to enhance chemoreception by more effectively elongating the algal phycosphere towards the nauplius. Compared with nauplii, *E. pileatus* early copepodites, being larger in size and negatively buoyant, beat appendages in a more complex, intermittent pattern to generate an r^{-1}-decay feeding current for displacing more water, indicating a trade-off among feeding, predator avoidance, and alga perception.

KEY WORDS: *Eucalanus pileatus* · Nauplii · Appendage beat pattern · Vortical feeding current · Remote detection · Chemoreception · Copepodites

1. INTRODUCTION

All copepods except a few parasitic species begin life as a nauplius (Fryer 1986). Just as copepods are considered the most numerous multicellular animals on earth (Humes 1994), so, too, copepod nauplii are believed to be the most abundant type of multicellular animal in existence (Fryer 1986). Despite being more abundant, copepod nauplii often suffer higher stage-specific mortality than copepodites or adults (Paffenhöfer 1970, Landry 1978, Eiane et al. 2002). Considering the significance of planktonic copepods in marine ecosystems and the fact that adult copepods eventually develop from nauplii, it is fundamentally important to investigate naupliar behavioral ecology, including swimming and feeding behaviors, predator–prey interactions, and nauplius–fluid interactions.

Nauplii of planktonic copepods exhibit species-specific and stage-specific swimming behaviors, including swimming continuously, swimming in a hop-like mode, and moving in a jump–sink fashion (Buskey 1994, van Duren & Videler 1995, Paffenhöfer et al. 1996, Titelman & Kiørboe 2003a), and these swimming behaviors correlate with naupliar feeding

*Corresponding author: hsjiang@whoi.edu

modes. Many calanoid nauplii that swim either continuously or in a hop-like mode create a feeding current to entrain prey; in contrast, some calanoid and many cyclopoid nauplii that move in a jump–sink fashion use ambush feeding to prey on motile prey (Paffenhöfer & Lewis 1989, Paffenhöfer et al. 1996, Henriksen et al. 2007, Bruno et al. 2012).

Motile behavior of copepod nauplii also affects their interactions with predators such as adult omnivorous copepods. Nauplii moving in a jump–sink fashion are more sensitive in detecting the hydrodynamic signal imposed by an approaching predator, thereby escaping earlier, than those swimming continuously (Titelman 2001, Titelman & Kiørboe 2003b, Jiang & Paffenhöfer 2004). Nauplii of *Acartia tonsa* tested in siphon flow required a 6 times higher threshold deformation rate to elicit jumping than *A. tonsa* adults, supporting the notion that nauplii suffer a greater predation risk than adults (Fields & Yen 1997).

Copepod nauplii have 3 pairs of appendages, the antennules (A1), the antennae (A2), and the mandibles (Md); 2 or 3 pairs of appendages are used for propulsion and feeding (Gauld 1959, Björnberg 1986, Paffenhöfer & Lewis 1989). Since they move in a low Reynolds number flow, copepod nauplii must coordinate movements of their appendages into a nonreciprocal pattern (Purcell 1977, Strickler 1984) for swimming and jumping (Andersen Borg et al. 2012, Gemmell et al. 2013, Lenz et al. 2015), jumping to attack and capture prey (Bruno et al. 2012), or generating a feeding current to entrain prey (Paffenhöfer & Lewis 1989). At low Reynolds numbers, copepod nauplii, e.g. *A. tonsa* nauplii (Wadhwa et al. 2014) and *Temora longicornis* nauplii (Kiørboe et al. 2014), jump by using a fast, breaststroke-like appendage beat pattern, imposing a potential dipole-like flow that attenuates with distance r as r^{-3}.

Calanoid nauplii such as *Eucalanus pileatus*, *E. crassus*, *T. longicornis, T. stylifera*, and *T. turbinata* create a feeding current (Paffenhöfer & Lewis 1989, Paffenhöfer et al. 1996, Andersen Borg et al. 2012, Kiørboe et al. 2014). Nauplii of *T. longicornis* beat all 3 pairs of appendages rhythmically to swim while creating a feeding current that attenuates with distance r as r^{-1} to r^{-2} (i.e. Stokeslet + stresslet) for optimized feeding efficiency but at an elevated risk to rheotactic predators (Andersen Borg et al. 2012, Kiørboe et al. 2014). By contrast, nauplii of *E. pileatus* beat only the A2 and the Md to create a feeding current (Paffenhöfer & Lewis 1989). Although trajectories of entrained algae and flow speeds at points have been measured for the feeding current created by a tethered *E. pileatus* nauplius, the spatial configuration and decay rate of the feeding current has not been quantified.

In this study, by using a high-speed microscale imaging system (HSMIS), micro-particle image velocimetry (μPIV) flow-field measurements were made to quantify the feeding current created by a free-swimming *E. pileatus* nauplius and to estimate potential ingestion rates under environmental food conditions. The HSMIS was also used to conduct quantitative microvideography of free-swimming *E. pileatus* nauplii capturing algae entrained into their feeding current, with a comparison with counterpart observations for free-swimming *E. pileatus* early copepodites. The study was conducted to shed light on the adaptive significance of naupliar feeding currents.

2. MATERIALS AND METHODS

Late naupliar stages of *Eucalanus pileatus*, one of the characteristic calanoids on the southeastern shelf of the USA (Bowman 1971), were observed in the present study. The nauplii were reared in the laboratory from eggs that originated from adult females or copepodites collected on the middle shelf off Savannah, GA. The nauplii were raised at ~21°C in the laboratory in 3.48 l screw-cap jars rotated at 0.2 rpm on a plankton wheel at a 14:10 h light:dark cycle. They were offered mainly the diatom *Thalassiosira weissflogii* (10–12 μm equivalent spherical diameter) and a much lesser amount of the large diatom *Rhizosolenia alata* (~35 μm cell width, 200–400 μm cell length) as food. Specifically, the nauplii were offered food at a concentration close to 46 μg C l^{-1} approximately 48 h before each round of observation. We determined that the food concentration decreased to a value in the range of 7–16 μg C l^{-1} due to feeding of the nauplii over the past 48 h. Food was then added, bringing the concentration to a value in the range of 43–67 μg C l^{-1}, and observation was conducted immediately after. This procedure ensured that the nauplii were quite hungry and eager to feed during each round of observation. Note that the food concentrations used in the present study were within the range of environmental phytoplankton abundances (2.4–240 μg C l^{-1}, Paffenhöfer & Lewis 1990). For comparison, early copepodites of *E. pileatus* were also observed following the same procedure. The development from late naupliar to early copepodite stages was accompanied by significant morphological changes in cephalic appendages as well as elongation in body shape (Fig. 1).

For conducting both μPIV and microvideography, high-speed high-resolution digital videos were taken

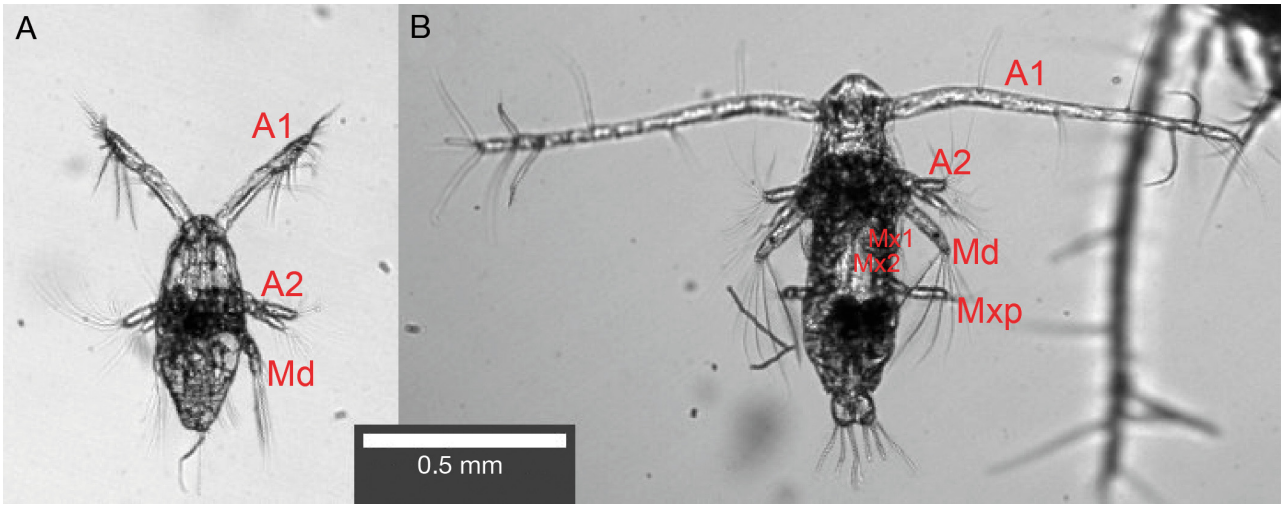

Fig. 1. Image stills of the ventral view of (A) a naupliar stage 6 (N6) and (B) a copepodite stage 1 (C1) of the copepod *Eucalanus pileatus*. The cephalic appendages are labeled as A1 (antennule), A2 (antenna), Md (mandible), Mx1 (maxillule), Mx2 (maxilla), and Mxp (maxilliped)

by using the HSMIS. The HSMIS consists of a Photron FASTCAM SA3 120K monochrome video camera that takes 1024 × 1024-pixel resolution images at a frame rate up to 2000 fps. The camera is mounted horizontally with a 175 mm focal length objective lens plus an infinity-corrected, long-working-distance microscope objective (4×/0.10 18.5 mm working distance) to yield a field-of-view of a vertically oriented area of ~4.4 × 4.4 mm. For microvideography, ~20 nauplii of stages N3 to N6 combined with food at the abovementioned concentration were held inside a 25 ml tissue culture flask; 3 such flasks were prepared consecutively, and videos were acquired at 1000 fps for nauplii in each flask. For µPIV, ~20 nauplii of stages N3 to N6 were put inside a 25 ml tissue culture flask filled with seawater seeded with 3 µm diameter polystyrene spheres; videos were subsequently obtained at 2000 fps for 2 such flasks prepared. A 1 W white LED light source was collimated to provide backlit illumination in which light was shined toward the camera through a prepared flask placed in front of the microscope objective. The field-of-view was focused at the center of the flask, which was at least 1 cm away from flask walls. All observations were made in a temperature-controlled room, held at ~21°C. The HSMIS of different optical specifications has been previously used for quantitative microvideography of protists (Jiang & Johnson 2017, Jiang et al. 2018) and µPIV measurements of suspension-feeding juvenile clams (Du Clos & Jiang 2018). The HSMIS has the advantage of achieving sharp imaging under low illumination.

The planar PIV technique has been applied to measure copepod-imposed flow fields since the late 1990s (e.g. van Duren et al. 1998). In a standard application of the planar PIV technique, a laser is used to form a thin laser sheet where tracer particles are illuminated, cutting through the fluid volume. Instead of using a thin laser sheet, the HSMIS uses a collimated LED light source to illuminate the fluid volume; the high-magnification optical setup of the HSMIS has a narrow depth-of-field that provides a well-focused thin slice (<100 µm) of tracer particles in the naupliar feeding current, making it feasible to do 2-dimensional µPIV (e.g. Gemmell et al. 2014). The original frame rate for taking videos for µPIV was 2000 fps; however, the resulting time interval between 2 consecutive images was too short to generate sufficient displacements of tracer particles. To solve this problem, each original brightfield video was subsampled at 200 fps, and then inverted via the ImageJ software before being imported into the DaVis v8.40 software (LaVision) for PIV processing. The pixels of the naupliar body were excluded from PIV vector calculations by applying an intensity threshold-based mask. Velocity fields were calculated by using cross-correlation of 2 consecutive frames in the video (i.e. the 'single frame' mode). Specifically, a multi-pass iteration algorithm was used with initial and final interrogation window sizes of 32 × 32 pixels and 16 × 16 pixels (69 × 69 µm), respectively, with a 50% overlap.

All high-speed digital videos were imported into the ImageJ software for measuring naupliar body

length (L), path-averaged speed (U_{ave}), net to gross displacement ratio (NGDR), and appendage beat frequency (f). The videos were further analyzed to determine the naupliar appendage beat pattern and the behavior of free-swimming *E. pileatus* nauplii capturing algae entrained into their feeding current. Rotation speed (ω) of the naupliar main body was calculated as the time derivative of the angle that is formed from the horizontal rightward direction to the direction of body orientation that is defined from the posterior tip to the anterior tip, with positive derivative values indicating counterclockwise rotation. For comparison, similar measurements and analyses were made for a few free-swimming *E. pileatus* early copepodites.

To assess whether the naupliar feeding current would entrain and capture enough food to cover metabolic cost and further support growth and development in the nutritionally dilute open ocean, the feeding current-induced potential ingestion rate was calculated and compared with the metabolic rate. Following Köster et al. (2008), at ~21°C the daily individual *E. pileatus* naupliar oxygen consumption (M_{O_2}, ml O_2 nauplius^{-1} d^{-1}) was calculated as:

$$M_{O_2} = 3.692 \times 10^{-4}\,(\mathrm{AFDW})^{0.781} \quad (1)$$

where AFDW is the ash-free dry weight (µg nauplius^{-1}), calculated as:

$$\mathrm{AFDW} = 8.054 \times 10^{-6}\,L^{1.997} \quad (2)$$

where L (µm) is the body length of the nauplius. M_{O_2} was converted from ml O_2 nauplius^{-1} d^{-1} to cal nauplius^{-1} d^{-1} by using the conversion factor 4.86 cal (ml O_2)$^{-1}$; AFDW was converted from µg nauplius^{-1} to cal nauplius^{-1} by using the conversion factor 5.0 × 10^{-3} cal µg^{-1}. The daily weight-specific metabolic rate (M, % d^{-1}) was then calculated as:

$$M = \frac{4.86 \times M_{O_2}}{5.0 \times 10^{-3} \times \mathrm{AFDW}} \times 100 \quad (3)$$

Next, the feeding current-induced potential ingestion rate (I_{FC}, µg C nauplius^{-1} d^{-1}) was calculated as:

$$I_{FC} = 10^{-3}\,Q\,C_e \quad (4)$$

where Q is the naupliar feeding current-induced volume flux (ml nauplius^{-1} d^{-1}) towards the ventral surface of the nauplius and C_e is the environmental food concentration (µg C l^{-1}). I_{FC} was converted from µg C nauplius^{-1} d^{-1} to cal nauplius^{-1} d^{-1} by using the conversion factor 1.099 × 10^{-2} cal (µg C)$^{-1}$. The daily weight-specific feeding current-induced potential ingestion rate (I, % d^{-1}) was then calculated as:

$$I = \frac{1.099 \times 10^{-2} \times I_{FC}}{5.0 \times 10^{-3} \times \mathrm{AFDW}} \times 100 \quad (5)$$

3. RESULTS

3.1. Swimming behavior and kinematics

Nauplii of *Eucalanus pileatus* vibrate their A2 and Md to swim while creating a feeding current. Their A1 do not vibrate at all, but A2 and Md always beat continuously without stopping at 17.8 ± 1.6 (SD) Hz (Table 1). The nauplii usually adopt a horizontal to upside-down orientation (Fig. 2A), but can swim in any direction (Fig. 2B). Their swimming direction does not correlate with body orientation ($R^2 < 0.001$, Fig. 2C) and therefore is not limited by a specific body orientation. In this sense, they have extremely versatile swimming capabilities.

Compared with swimming under simulated environmental food conditions, *E. pileatus* nauplii in a dense suspension of 3 µm diameter polystyrene spheres swim at slightly reduced (though not statistically significant) mean swimming speed and NGDR (Fig. 3A–C), but beat their appendages at a statistically significantly lower mean frequency (Student's t-test, $p = 0.040$; Fig. 3D, Tables 1 & 2). Despite these kinematic differences, the naupliar swimming behavior and appendage beat pattern seem unchanged.

Early copepodites of *E. pileatus* swim in a hover-and-sink pattern, while adopting a horizontal to

Table 1. Statistics of observed events of swimming by copepod nauplii of *Eucalanus pileatus* under simulated environmental food conditions. NGDR: net to gross displacement ratio

	Body length (L) (µm)	Total duration (ms)	Beat duration as % of total duration	Path-averaged speed (U_{ave}) mm s^{-1}	L s^{-1}	NGDR	Beat frequency (f) (Hz)
Mean ± SD	559 ± 64	3141.1 ± 1771.6	100 ± 0	1.5 ± 0.5	2.8 ± 0.9	0.567 ± 0.252	17.8 ± 1.6
Range	429–628	682.0–5456.0	100–100	0.7–2.5	1.7–4.3	0.216–0.961	14.7–20.4
n	16	16	16	16	16	16	16

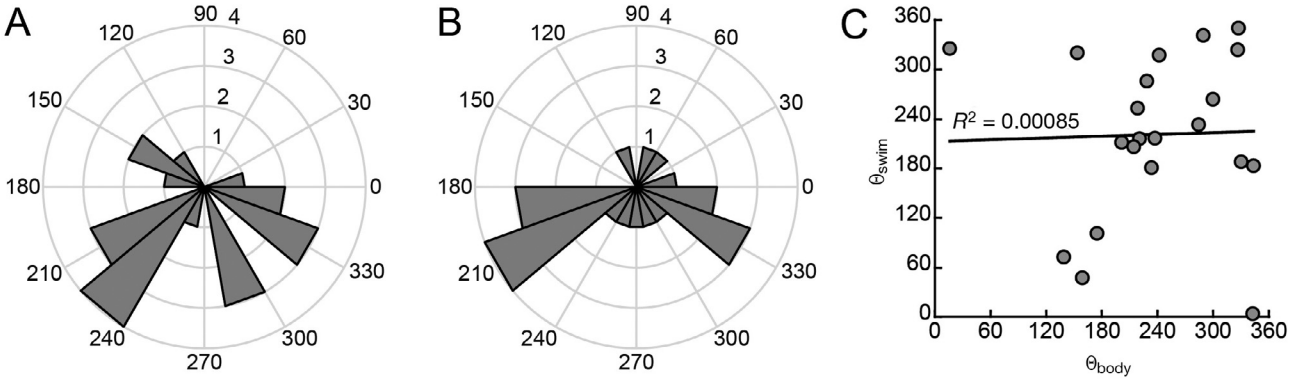

Fig. 2. Frequency distributions of (A) body orientation, θ_{body}, and (B) swimming direction, θ_{swim}, for *Eucalanus pileatus* nauplii. (C) θ_{swim} versus θ_{body}. Body orientation is defined as the direction from naupliar posterior tip to anterior tip

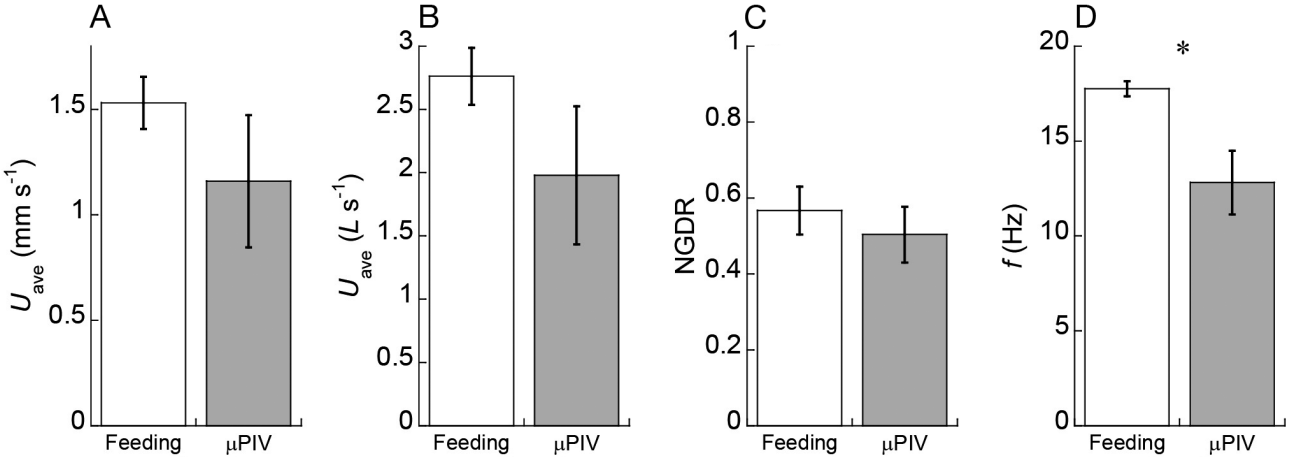

Fig. 3. Comparison of naupliar swimming kinematics: (A) path-averaged swimming speed (U_{ave}, mm s^{-1}), (B) path-averaged swimming speed (U_{ave}, L s^{-1}, where L is body length), (C) net to gross displacement ratio (NGDR), and (D) appendage beat frequency (f, Hz), under 2 conditions: (1) under simulated environmental food conditions, i.e. feeding, and (2) in a dense, 3 µm diameter polystyrene sphere suspension, i.e. micro-particle image velocimetry (µPIV). *: significantly different (p = 0.040). Error bars represent standard errors

upright orientation. The copepodites hover when beating their appendages at frequencies of 24.3 ± 3.0 Hz with durations of 395 ± 161 ms (Table 3). Once they stop beating their appendages, they sink immediately at speeds of 0.84 ± 0.42 mm s^{-1}, indicating that they are negatively buoyant; sinking lasts 180 ± 89 ms (Table 3). On average, they spend 75% of the time beating their appendages (Table 3). The copepodites have statistically significantly higher appendage beat frequencies than the nauplii (Student's *t*-test, p = 0.018; Tables 1 & 3). The latter 2 results are similar to those obtained previously by Paffenhöfer & Lewis (1989).

Table 2. Statistics of observed events of swimming by copepod nauplii of *Eucalanus pileatus* in a dense, 3 µm diameter polystyrene sphere suspension (i.e. micro-particle image velocimetry experiments). NGDR: net to gross displacement ratio

	Body length (L) (µm)	Total duration (ms)	Beat duration as % of total duration	Path-averaged speed (U_{ave}) mm s^{-1}	L s^{-1}	NGDR	Beat frequency (f) (Hz)
Mean ± SD	573 ± 33	1865.3 ± 922.4	100 ± 0	1.2 ± 0.7	2.0 ± 1.2	0.504 ± 0.165	12.8 ± 3.8
Range	548–614	506.0–2728.0	100–100	0.6 – 2.3	0.9 – 3.9	0.355–0.784	7.5–16.7
n	5	5	5	5	5	5	5

Table 3. Statistics of observed events of swimming by early copepodites of *Eucalanus pileatus* under simulated environmental food conditions. NGDR: net to gross displacement ratio

	Prosome length (L) (µm)	Total duration (ms)	Beat duration as % of total duration	Duration of 1 non-stop hovering (ms)	Duration of 1 non-stop sinking (ms)	Sinking speed (U_{sink}) (mm s^{-1})	NGDR	Beat frequency (f) (Hz)
Mean ± SD	765 ± 94	3592 ± 1472	75 ± 10	395 ± 161	180 ± 89	0.84 ± 0.42	0.215 ± 0.101	24.3 ± 3.0
Range	639–863	2002–5148	64–88	169–767	84–397	0.41–1.42	0.107–0.332	20.8–27.8
n	4	4	4	19	21	4	4	4

3.2. Appendage beat pattern

Nauplii of *E. pileatus* beat their appendages in a 'double draw-and-cut' pattern (see Video Group S1 [Events A and B] in the Supplement at www.int-res.com/articles/suppl/m638p051_supp/), in which the Md oscillates rapidly between the A2 and the posterior surface, with high precision (Fig. 4). That is, 2 sets of 'draw-and-cut' movements are operated alternately and in antiphase by an A2–Md combination and an Md–posterior surface combination. Specifically, right after touching each other flatly, the A2 and the Md rapidly pull away from each other, drawing in water between themselves; at their farthest distance from each other, they halt suddenly, turn rapidly by 90 degrees, and approach each other by cutting through the water with their narrow ends, i.e. not pushing out much water. As they approach each other very closely, they again come to a sudden halt and again turn rapidly by 90 degrees, thereby facing each other with their flat ends; then they rapidly pull away from each other, starting another beat cycle. In

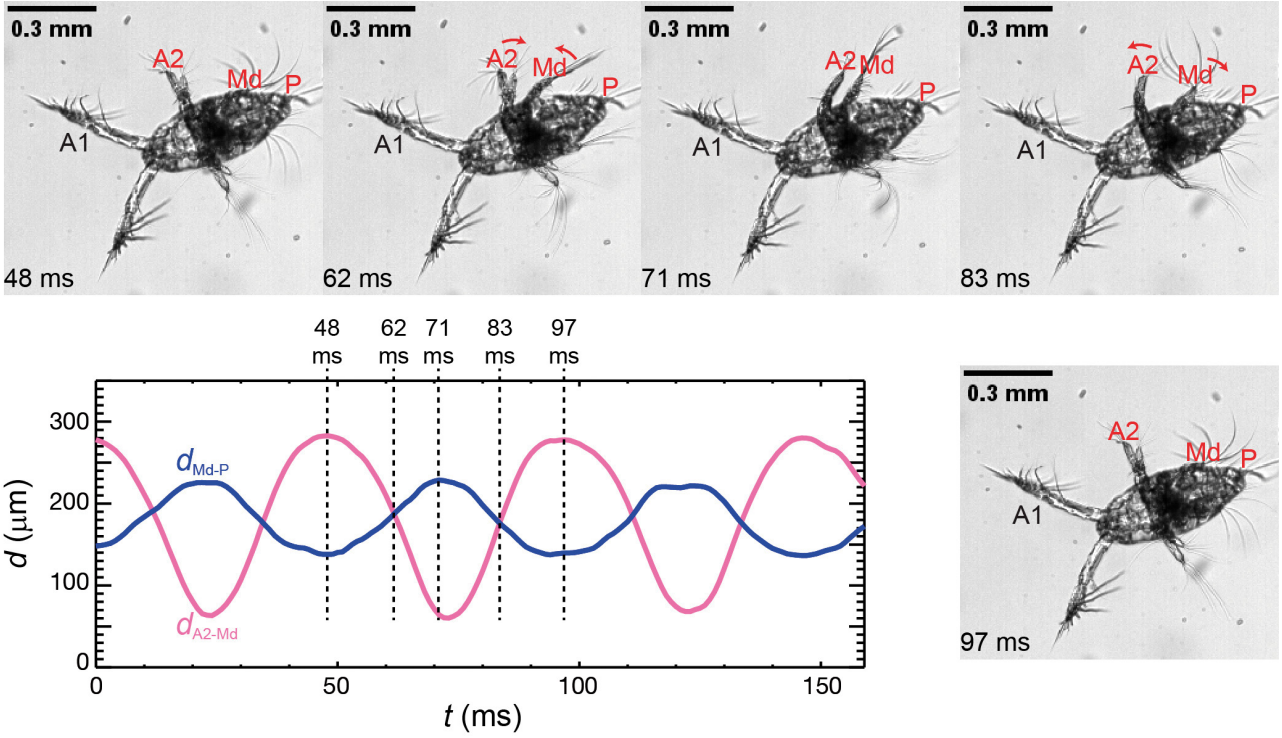

Fig. 4. Beat cycles analyzed for a nauplius performing a 'double draw-and-cut' appendage beat pattern (Event A in Video Group S1). The line plot is for distances between the A2 (see Fig. 1 for definitions) tip and the Md tip, $d_{A2\text{-}Md}$, and between the Md tip and the posterior tip, $d_{Md\text{-}P}$, over time. The image sequence shows the progression of 1 beat cycle. At 48 ms, the Md flatly touches the posterior surface, where $d_{Md\text{-}P}$ reaches minimum and $d_{A2\text{-}Md}$ reaches maximum. At 62 ms, the Md departs from the posterior surface, while the Md and the A2 move toward each other. At 71 ms, the Md and the A2 effectively touch each other flatly, where $d_{A2\text{-}Md}$ reaches minimum and $d_{Md\text{-}P}$ reaches maximum. At 83 ms, the Md and the A2 pull away from each other, while the Md moves toward the posterior surface. At 97 ms, the Md flatly touches the posterior surface, where $d_{Md\text{-}P}$ reaches minimum and $d_{A2\text{-}Md}$ reaches maximum

the Md–posterior surface combination, the 'draw-and-cut' maneuver is performed only by the Md.

In contrast, early copepodites of *E. pileatus* beat their appendages in a more complex pattern (Video Group S2). Although the maxilliped (Mxp) and the A2 beat oppositely to form an 'open and close' pattern, between them there are the Md, the maxillule (Mx1), and the maxilla (Mx2), all moving simultaneously in their own ways, and none of these appendages touches the body surface of the copepodite. This observation is similar to what has been described previously by Strickler (1984) for adult females of *E. pileatus*.

3.3. Naupliar feeding current

Nauplii of *E. pileatus* create a vortical feeding current by beating their appendages in the 'double draw-and-cut' pattern (Video Group S3). The 1 beat cycle-averaged flow field consists of a core flow that is directed towards the ventral surface of the nauplius (Fig. 5A). A clockwise vortex is located to the anterior side of the nauplius and left of the core flow, while an anticlockwise vortex is located to the posterior side and right of the core flow; thus, both vortices reinforce the core flow. Both vortices are viscous in nature as evidenced by the observation that both vortex centers are well separated from the magnitude maxima of vorticity (Fig. 5B). Within each beat cycle, both pulling-apart movements, operated alternately and in antiphase by the A2–Md combination and by the Md–posterior surface combination, contribute to generating the core flow towards the ventral surface of the nauplius (Video A in Video Group S3); the effective touching between the A2 and the Md squeezes the water in-between, thereby creating the clockwise viscous vortex that moves away from the ventral surface towards the anterior side of the nauplius, while the effective touching between the Md and the posterior surface creates the

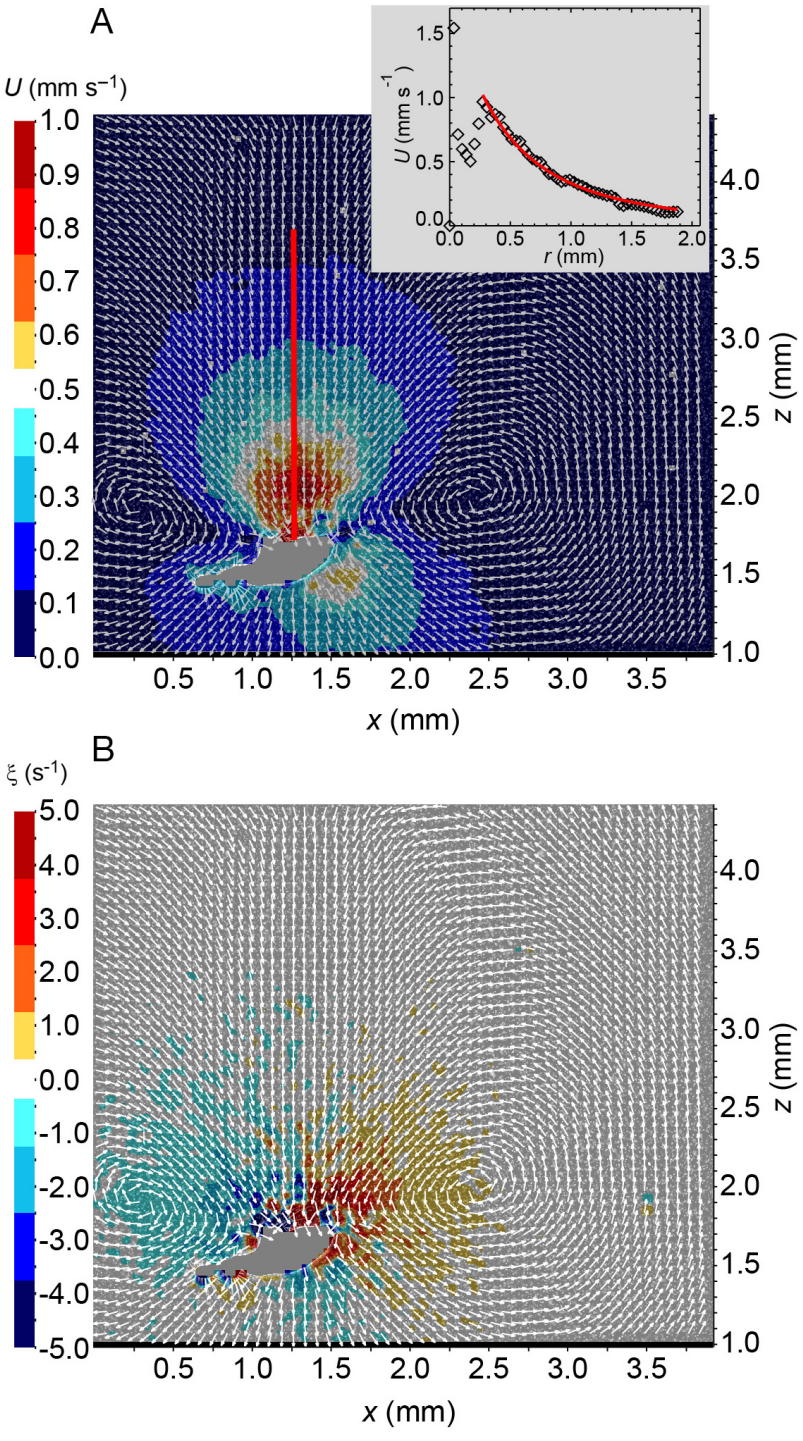

Fig. 5. Free-swimming *Eucalanus pileatus* nauplius creating a vortical feeding current (Video Group S3). Shown here is the 1 beat cycle-averaged flow field from micro-particle image velocimetry (μPIV) measurements: equal-length velocity vectors overlapping (A) with velocity magnitude color contours and (B) with vorticity color contours. The inset in A shows the spatial decay of the flow velocity magnitude along the solid red line, i.e. the red line in the inset represents an r^{-3} fit to the decay part of the velocity data (diamonds), where r is distance to the ventral surface of the nauplius. The volume flux of the core flow towards the ventral surface of the nauplius is ~9 ml d^{-1} (0.7×10^6 naupliar body volumes per day)

Table 4. Statistics of daily weight-specific metabolic rate (M) and daily weight-specific feeding current-induced potential ingestion rate (I) of copepod nauplii of *Eucalanus pileatus* under environmental food concentrations of the open ocean

	Body length (L) (µm)	Volume flux towards naupliar ventral surface (Q) (ml nauplius^{-1} d^{-1})	M (% d^{-1})	I (% d^{-1}) calculated at 3 environmental food concentrations (C_e)		
				2.4 µg C l^{-1}	24 µg C l^{-1}	240 µg C l^{-1}
Mean ± SD	589 ± 35	11.2 ± 2.5	28.8 ± 0.8	2.2 ± 0.7	22.1 ± 7.5	221.0 ± 75.2
Range	549–614	8.8–13.7	28.3–29.7	1.6–3.0	15.6–30.3	155.9–303.4
n	3	3	3	3	3	3

anticlockwise viscous vortex that leaves the ventral surface towards the posterior side of the nauplius (Videos B & C in Video Group S3). The core flow of the naupliar feeding current attenuates with distance r as r^{-3} (Fig. 5A inset). In total, 5 cases were obtained and analyzed, all displaying the above-described vortical flow pattern. In 3 of these cases, the focal plane coincided approximately with the sagittal plane of the nauplius, making it possible to estimate from µPIV measurements the volume flux of the core flow towards the ventral surface of the nauplius: 9–14 ml d^{-1} (0.7–1.6 ×10^6 naupliar body volumes per day), comparable to the volume-swept-clear values of 2–10 ml d^{-1} obtained previously by Paffenhöfer & Knowles (1978).

At low environmental food concentrations in the range of 2.4–24 µg C l^{-1}, the daily weight-specific feeding current-induced potential ingestion rate cannot cover the daily weight-specific metabolic rate of ~28.8% d^{-1} (Table 4). At a high environmental food concentration of 240 µg C l^{-1}, the daily weight-specific feeding current-induced potential ingestion rate reaches ~221.0% d^{-1}, which is more than enough to cover the daily weight-specific metabolic rate (Table 4).

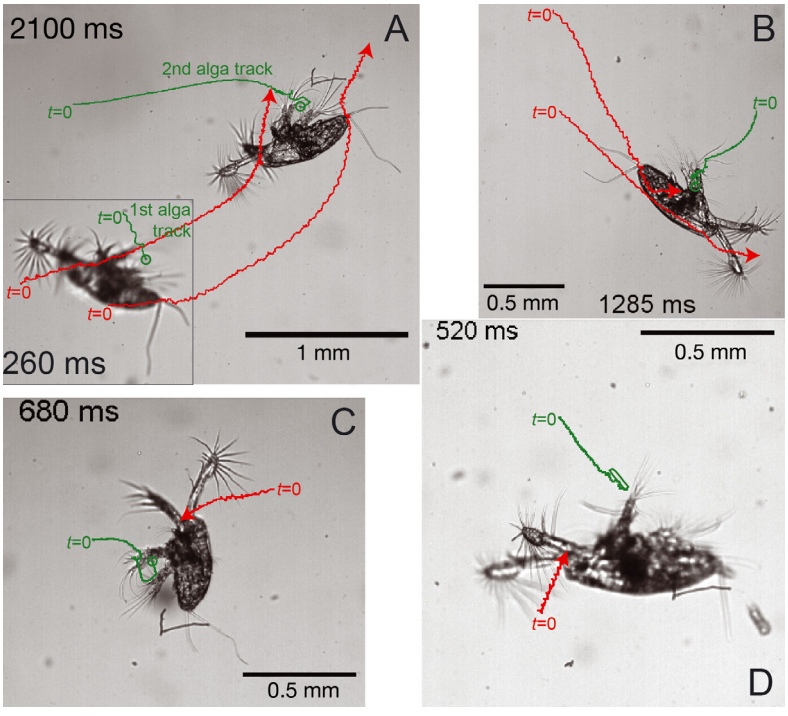

Fig. 6. Image frames extracted from videos (Events A–D in Video Group S4) illustrating free-swimming *Eucalanus pileatus* nauplii using a combined action of a feeding current and whole-body swimming motion to displace algae from various directions towards their mouthpart zone between the A2 (see Fig. 1 for definitions) and the Md for ensuing capture. Each green line marks the trajectory of an entrained alga (marked by green circles in A, B, and C, and a green rod in D). In A and B, the 2 red arrows are respectively the trajectories of the posterior and anterior tips of the nauplius. In C and D, the red arrow is the trajectory of the anterior tip of the nauplius

3.4. Behavior for capturing algae

Free-swimming *E. pileatus* nauplii use a combined action of a feeding current and whole-body swimming motion to displace algae towards their mouthpart zone between the A2 and the Md for ensuing capture (Fig. 6; Video Group S4). A nauplius can maintain a suitable swimming direction and body orientation while generating a feeding current in a different direction, such that the combined action directs an entrained alga to the mouthpart zone of the nauplius (Fig. 6A inset, Fig. 7B,C & Event A in Video Group S4; Fig. 6C & Event C in Video Group S4; Fig. 6D & Event D in Video Group S4). Moreover, depending on their relative positions, a nauplius can modify its swimming direction and make suitable nonrandom turns to meet an alga that is entrained into its feeding current (Fig. 7D–F & Event A in Video Group S4; Fig. 8B–D & Event B in Video Group S4).

For an event in which the nauplius turns toward the incoming alga, the time history of naupliar body rotation speed reflects the reaction of the nauplius to the alga. In Event A of Video Group S4 (Fig. 7D–F), the nauplius turns toward the second alga before intercepting and capturing it. At ~1660 ms while turning toward the alga (Fig. 7E), the nauplius attains maximum body rotation speed (marked by a short time duration Δt_1 in Fig. 7A); at this instant, the alga is ~362 µm away from the nearest naupliar seta (distance marked by the white line segment in Fig. 7E); this distance can be taken as the reaction distance of the nauplius to the alga, and the remote detection distance can be even longer. Similarly, for Event B of Video Group S4, a reaction distance of ~493 µm can be determined for the nauplius to the incoming alga (Fig. 8).

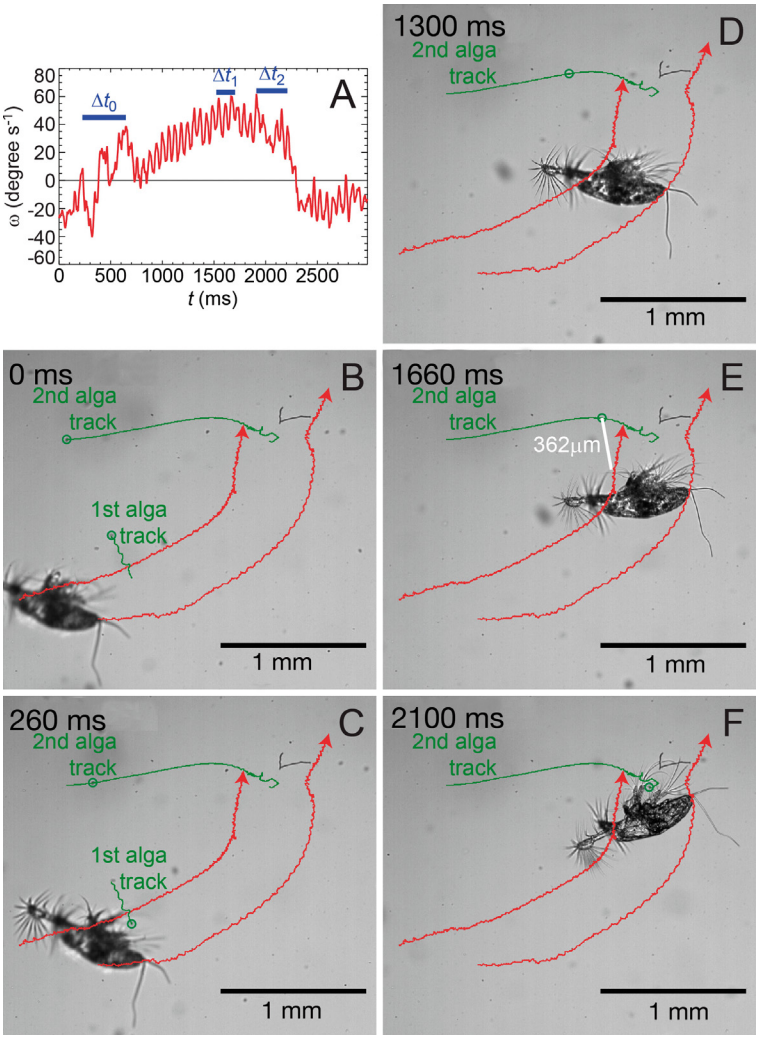

Fig. 7. Time-course image sequence illustrating a free-swimming *Eucalanus pileatus* nauplius entraining and capturing 2 algae one by one (Event A in Video Group S4), along with (A) time history of body rotation speed (ω) of the nauplius. (B) Initially, the nauplius swims horizontally rightward while creating a feeding current to entrain the first alga. (C) At ~260 ms, the first alga arrives at the mouthpart zone. The nauplius maneuvers to capture the alga while rotating its body quickly and irregularly during a short time duration Δt_0 as shown in A. After that, the nauplius moves on. (D) The nauplius turns toward the second alga. (E) At ~1660 ms while turning toward the alga, the nauplius attains maximum body rotation speed (as marked by Δt_1 in A); the white line segment connecting from the alga to the nearest naupliar seta measures ~362 µm, which can be taken as the reaction distance of the nauplius to the alga; the remote detection distance can be even longer. (F) At ~2100 ms, the second alga arrives at the mouthpart zone. The nauplius maneuvers to capture the alga while rotating its body quickly and irregularly during Δt_2 as shown in A. See Fig. 6 for explanations of green lines and red arrows

By contrast, free-swimming *E. pileatus* early copepodites use a feeding current to entrain and capture algae (Video Group S5). As already mentioned, the copepodites swim in a hover-and-sink fashion. During hovering, they create a downward feeding current by beating their appendages to push against their excess weight. During sinking, they stop beating their appendages and drag down with their sinking body a substantial amount of surrounding water including embedded algae. They perform multiple rounds of hover-and-sink to displace algae towards their mouthpart zone for ensuing capture or rejection. During 1 event, a copepodite was observed to beat its right- and left-side appendages subtly differently and adjust beating directions slightly in response to 2 algae being entrained from different sides (Event A in Video Group S5; Fig. 9A). In another event, a copepodite was observed to pause and then restart beating of appendages aiming at a slightly different direction in response to an entrained alga (Event B in Video Group S5; Fig. 9B).

4. DISCUSSION

4.1. Naupliar feeding-current generation mechanism

Eucalanus pileatus nauplii use a novel 'double draw-and-cut' appendage beat pattern that is nonreciprocal to create a vortical feeding current at a Reynolds number (*Re*) of ~0.8. Each time when the A2–Md pair or the Md–posterior surface

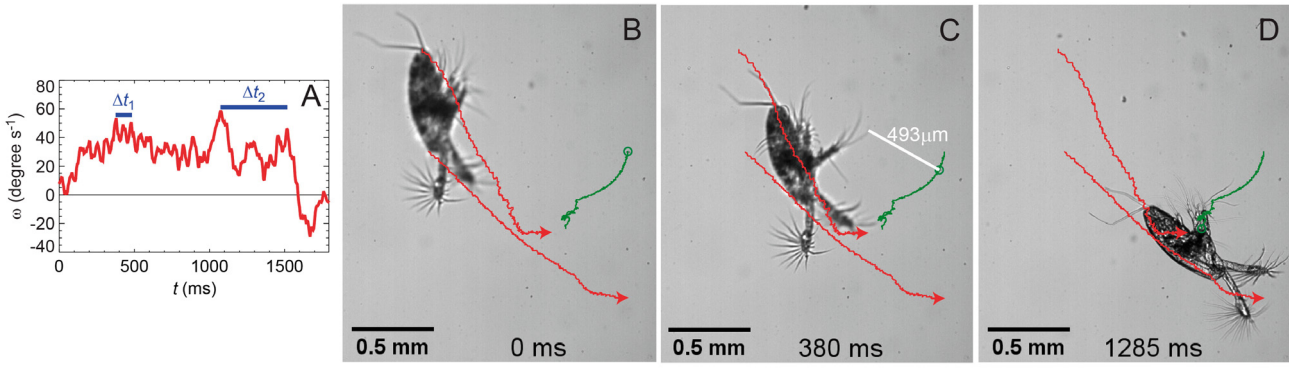

Fig. 8. Time-course image sequence illustrating a free-swimming *Eucalanus pileatus* nauplius entraining and capturing an alga (Event B in Video Group S4), along with (A) time history of body rotation speed (ω) of the nauplius. (B) Initially, the nauplius is in an upside-down posture while beating its appendages to generate a feeding current, and the alga is located a horizontal distance away. Later on, the nauplius turns to an oblique posture while using its feeding current to eventually displace the alga to its mouthpart zone for ensuing capture. (C) At ~380 ms while turning toward the alga, the nauplius attains maximum body rotation speed (as marked by Δt_1 in A); the white line segment connecting from the alga to the nearest naupliar seta measures ~493 μm, which can be taken as the reaction distance of the nauplius to the alga; the remote detection distance can be even longer. (D) At ~1285 ms, the alga arrives at the mouthpart zone. The nauplius maneuvers to capture the alga while rotating its body quickly and irregularly during Δt_2 as shown in A. See Fig. 6 for explanations of green lines and red arrows

pair is pulled open, mass conservation demands that water must rush into the opening gap, thereby generating the core flow towards the ventral surface of the nauplius. The alternate and antiphase operations between the A2–Md pair and the Md–posterior surface pair ensure that there is always a branch of water flow towards the ventral surface. The asymmetry in appendage posture contrasting a 'draw' phase and a 'cut' phase ensures that more water is drawn in during a 'draw' phase than is squeezed out during a 'cut' phase.

Moreover, the core flow is reinforced laterally by 2 viscous vortices that are generated alternately due to the effective touching and squeezing between the A2 and the Md and between the Md and the posterior surface. Similar to the dimensionless 'jump number' defined to characterize the impulsiveness of copepod jumping (Jiang & Kiørboe 2011), a dimensionless 'squeeze number' can be defined to characterize the impulsiveness of appendage touching and squeezing:

$$N_{\text{squeeze}} \equiv \frac{\tau}{L^2/(4\nu)} \quad (6)$$

where τ is squeeze duration (= 1/[2*f*], where *f* is mean frequency of appendage beating [=17.8 Hz, Table 1]), *L* is mean body length (=559 μm, Table 1),

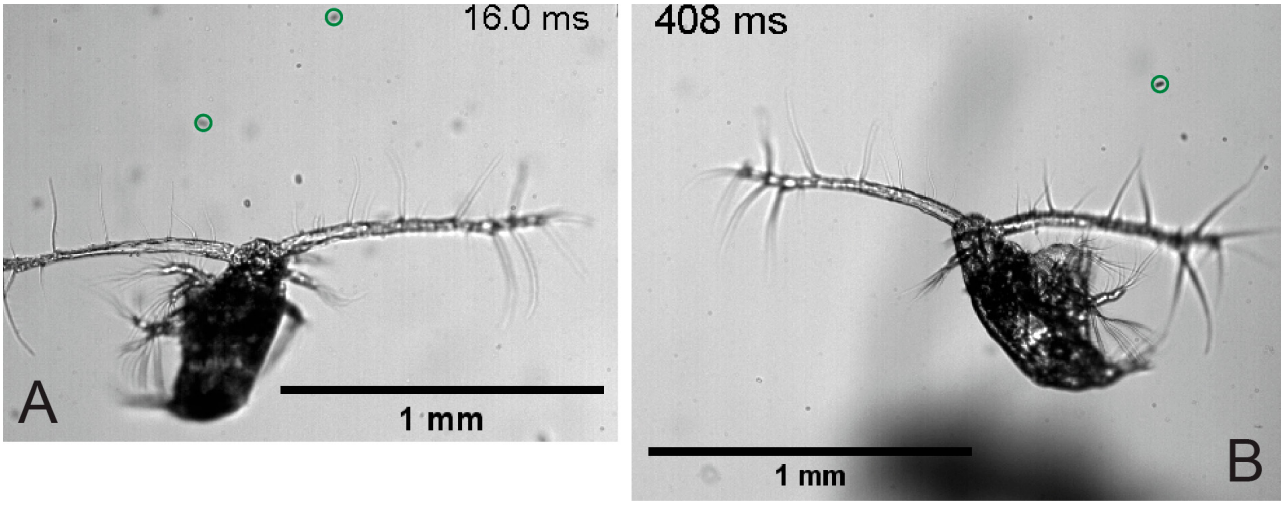

Fig. 9. Image frames extracted from videos of free-swimming *Eucalanus pileatus* early copepodites entraining and capturing/rejecting algae. (A) From Event A of Video Group S5. (B) From Event B of Video Group S5. The image frames illustrate the moment right before the copepodite starts a new round of its feeding current to finally draw in an alga (marked by a green circle) to its mouthpart zone. See Section 3.4 for detailed description

and ν is seawater kinematic viscosity (=1.028×10^{-6} m^2 s^{-1}, for seawater at 21°C, salinity 36 ppt, and 1 normal atmosphere). $N_{squeeze}$ is the ratio of squeeze duration and viscous time scale, and for values of order 1 or less, the induced flow will be in the form of a viscous vortex. For the nauplii, $N_{squeeze}$ is ~0.37, indicating that the squeezing-induced flow is in the form of a viscous vortex.

4.2. Adaptive significance of the naupliar feeding current

The 'double draw-and-cut' appendage beat pattern allows nauplii of *E. pileatus* to create a vortical feeding current that decays with distance r as r^{-3}. This behavior was probably selected for to bring 2 major adaptive values to the nauplii, and is thereby important for their survival. First, the spatially fast-attenuating naupliar feeding current fulfills its main function to transport entrained algae to the naupliar mouthpart zone for ensuing capture, while producing a spatially limited hydrodynamic disturbance that a rheotactic predator may have difficulty to detect. The volume flux transported by the feeding current towards the ventral surface of the nauplius has been measured to be $0.7–1.6 \times 10^6$ naupliar body volumes per day, conforming to the general requirement on zooplankton specific clearance rates in a nutritionally dilute ocean environment (Hansen et al. 1997, Kiørboe 2011, Kiørboe & Jiang 2013). In spite of that, nauplii are likely hungry most of the time when encountering a low environmental food concentration in the range of 2.4–40 µg C l^{-1}. At a relatively higher concentration >40 µg C l^{-1} the feeding current-induced potential ingestion rate can be large enough to cover the metabolic rate and further support growth and development.

Nevertheless, the present HSMIS observation has shown that a free-swimming *E. pileatus* nauplius can react to a remotely located alga that is being entrained into its feeding current by adjusting its swimming direction and making suitable nonrandom turns to meet the alga. The reaction distance is likely in the range of 300–500 µm. This high-accuracy behavior suggests remote detection, presumably via chemoreception, of the entrained alga by the nauplius, thereby enhancing food encounters. This observation points to the second adaptive value of the naupliar feeding current: compared with a Stokeslet-like, adult copepod feeding current with an r^{-1} decay (Jiang et al. 2002), the r^{-3} decay of a naupliar feeding current makes it more effective to elongate the algal phycosphere towards the nauplius, ahead of the arrival of the entrained alga itself. When arriving at the edge of a naupliar feeding current, an alga will travel rather slowly because of the spatial limitation of the naupliar feeding current; however, the algal phycosphere that is closer to the nauplius will experience significantly higher flow because of the r^{-3} decay. Thus, the slow-moving alga is under the control of the naupliar feeding current, while the significantly elongated algal phycosphere allows the nauplius to remotely detect the alga and respond accordingly.

4.3. Transition from late nauplii to early copepodites

The transition from late nauplii to early copepodites in *E. pileatus* is accompanied by consistent changes in size, morphology, appendage beat pattern, excess weight, and feeding current structure. Copepodites are larger in size and therefore require higher absolute clearance rates to satisfy the general requirement for zooplankton specific clearance rates, i.e. to be on the order of 1.0×10^6 body volumes per day (Hansen et al. 1997, Kiørboe 2011, Kiørboe & Jiang 2013). Copepodites have more pairs of mouthpart appendages than nauplii; thus, copepodites do not use the 'double draw-and-cut' appendage beat pattern that works for nauplii, but rather use a drag-based appendage beat pattern that generally involves asymmetric power and recovery strokes (Gauld 1966). Nauplii beat their appendages 100% of time, while copepodites beat ~75% of time, and copepodites beat their appendages at higher frequencies than nauplii. By not moving their cephalic appendages for ~25% of time, the sinking copepodite stages can perceive predators better, especially using the 3-dimensionally oriented setae on the tips of their A1. Moreover, an intermittent appendage beat pattern can reduce, in a time-averaging sense, the overall level of hydrodynamic signals detectable to rheotactic predators. Probably because of their lipid content, nauplii are neutrally buoyant, as also revealed by the r^{-3} decay of their vortical feeding current; in contrast, copepodites are negatively buoyant as revealed by their hover-and-sink behavior. When hovering, copepodites create a downward feeding current by beating appendages to push against their excess weight. This wide, cone-shaped, first-order (i.e. r^{-1} decay) feeding current increases copepodite clearance rates, making it possible to meet the general requirement of zooplankton-

specific clearance rates in a nutritionally dilute ocean environment (Conover 1968). The copepodite feeding current is more powerful and efficient in concentrating food particles but also hydrodynamically more detectable than the naupliar feeding current. Also, as discussed above, the r^{-1} decay of the copepodite feeding current can be less effective in facilitating chemoreception of entrained algae than the r^{-3} decay of the naupliar feeding current. Thus, to summarize, the various changes accompanying the transition from late nauplii to early copepodites in *E. pileatus* may indicate a trade-off among feeding, predator avoidance, and alga perception.

Acknowledgements. This work was supported by National Science Foundation (NSF) grants OCE-1433979 and OCE-1559062 to H.J.; G.A.P. was supported by NSF grant OCE-8723174. We thank 3 anonymous reviewers for providing helpful and constructive comments that improved the manuscript.

LITERATURE CITED

Andersen Borg CM, Bruno E, Kiørboe T (2012) The kinematics of swimming and relocation jumps in copepod nauplii. PLOS ONE 7:e47486

Björnberg TKS (1986) Aspects of the appendages in development. Syllogeus 58:51–66

Bowman TE (1971) The distribution of calanoid copepods off the southeastern United States between Cape Hatteras and Southern Florida. Smithson Contrib Zool 96:1–58

Bruno E, Andersen Borg CM, Kiørboe T (2012) Prey detection and prey capture in copepod nauplii. PLOS ONE 7: e47906

Buskey EJ (1994) Factors affecting feeding selectivity of visual predators on the copepod *Acartia tonsa*: locomotion, visibility and escape responses. Hydrobiologia 292-293:447–453

Conover RJ (1968) Life in a nutritionally dilute environment. Am Zool 8:107–118

Du Clos KT, Jiang H (2018) Overcoming hydrodynamic challenges in suspension feeding by juvenile *Mya arenaria* clams. J R Soc Interface 15:20170755

Eiane K, Aksnes DL, Ohman MD, Wood S, Martinussen MB (2002) Stage-specific mortality of *Calanus* spp. under different predation regimes. Limnol Oceanogr 47:636–645

Fields DM, Yen J (1997) The escape behavior of marine copepods in response to a quantifiable fluid mechanical disturbance. J Plankton Res 19:1289–1304

Fryer G (1986) Structure, function and behavior and the elucidation of evolution in copepods and other crustaceans. Syllogeus 58:150–157

Gauld DT (1959) Swimming and feeding in crustacean larvae: the nauplius larva. Proc Zool Soc Lond 132:31–50

Gauld DT (1966) The swimming and feeding of planktonic copepods. In: Barnes H (ed) Some contemporary studies in marine science. George Allen & Unwin Ltd., London, p 313–334

Gemmell BJ, Sheng J, Buskey EJ (2013) Compensatory escape mechanism at low Reynolds number. Proc Natl Acad Sci USA 110:4661–4666

Gemmell BJ, Jiang H, Buskey EJ (2014) A new approach to micro-scale particle image velocimetry (μPIV) for quantifying flows around free-swimming zooplankton. J Plankton Res 36:1396–1401

Hansen PJ, Bjørnsen PK, Hansen BW (1997) Zooplankton grazing and growth: scaling within the 2–2,000-μm body size range. Limnol Oceanogr 42:687–704

Henriksen CI, Saiz E, Calbet A, Hansen BW (2007) Feeding activity and swimming patterns of *Acartia grani* and *Oithona davisae* nauplii in the presence of motile and non-motile prey. Mar Ecol Prog Ser 331:119–129

Humes AG (1994) How many copepods? Hydrobiologia 292-293:1–7

Jiang H, Johnson MD (2017) Jumping and overcoming diffusion limitation of nutrient uptake in the photosynthetic ciliate *Mesodinium rubrum.* Limnol Oceanogr 62:421–436

Jiang H, Kiørboe T (2011) The fluid dynamics of swimming by jumping in copepods. J R Soc Interface 8:1090–1103

Jiang H, Paffenhöfer GA (2004) Relation of behavior of copepod juveniles to potential predation by omnivorous copepods: an empirical-modeling study. Mar Ecol Prog Ser 278:225–239

Jiang H, Osborn TR, Meneveau C (2002) Chemoreception and the deformation of the active space in freely swimming copepods: a numerical study. J Plankton Res 24: 495–510

Jiang H, Kulis DM, Brosnahan ML, Anderson DM (2018) Behavioral and mechanistic characteristics of the predator-prey interaction between the dinoflagellate *Dinophysis acuminata* and the ciliate *Mesodinium rubrum.* Harmful Algae 77:43–54

Kiørboe T (2011) How zooplankton feed: mechanisms, traits and trade-offs. Biol Rev Camb Philos Soc 86:311–339

Kiørboe T, Jiang H (2013) To eat and not be eaten: optimal foraging behavior in suspension feeding copepods. J R Soc Interface 10:20120693

Kiørboe T, Jiang H, Gonçalves RJ, Nielsen LT, Wadhwa N (2014) Flow disturbances generated by feeding and swimming zooplankton. Proc Natl Acad Sci USA 111: 11738–11743

Köster M, Krause C, Paffenhöfer GA (2008) Time-series measurements of oxygen consumption of copepod nauplii. Mar Ecol Prog Ser 353:157–164

Landry MR (1978) Predatory feeding behavior of a marine copepod, *Labidocera trispinosa.* Limnol Oceanogr 23: 1103–1113

Lenz PH, Takagi D, Hartline DK (2015) Choreographed swimming of copepod nauplii. J R Soc Interface 12: 20150776

Paffenhöfer GA (1970) Cultivation of *Calanus helgolandicus* under controlled conditions. Helgol Wiss Meeresunters 20:346–359

Paffenhöfer GA, Knowles SC (1978) Feeding of marine planktonic copepods on mixed phytoplankton. Mar Biol 48:143–152

Paffenhöfer GA, Lewis KD (1989) Feeding behavior of nauplii of the genus *Eucalanus* (Copepoda, Calanoida). Mar Ecol Prog Ser 57:129–136

Paffenhöfer GA, Lewis KD (1990) Perceptive performance and feeding behavior of calanoid copepods. J Plankton Res 12:933–946

Paffenhöfer GA, Strickler JR, Lewis KD, Richman S (1996) Motion behavior of nauplii and early copepodid stages of marine planktonic copepods. J Plankton Res 18: 1699–1715

Purcell EM (1977) Life at low Reynolds number. Am J Phys 45:3–11

Strickler JR (1984) Sticky water: a selective force in copepod evolution. In: Meyers DG, Strickler JR (eds) Trophic interactions within aquatic ecosystems. AAAS Selected Symposium 85. American Association for the Advancement of Science. Westview Press, Boulder, CO, p 187–239

Titelman J (2001) Swimming and escape behavior of copepod nauplii: implications for predator-prey interactions among copepods. Mar Ecol Prog Ser 213:203–213

Titelman J, Kiørboe T (2003a) Motility of copepod nauplii and implications for food encounter. Mar Ecol Prog Ser 247:123–135

Titelman J, Kiørboe T (2003b) Predator avoidance by nauplii. Mar Ecol Prog Ser 247:137–149

van Duren LA, Videler JJ (1995) Swimming behaviour of developmental stages of the calanoid copepod *Temora longicornis* at different food concentrations. Mar Ecol Prog Ser 126:153–161

van Duren LA, Stamhuis EJ, Videler JJ (1998) Reading the copepod personal ads: increasing encounter probability with hydromechanical signals. Philos Trans R Soc B 353: 691–700

Wadhwa N, Andersen A, Kiørboe T (2014) Hydrodynamics and energetics of jumping copepod nauplii and copepodids. J Exp Biol 217:3085–3094

Editorial responsibility: Sigrun Jónasdóttir, Charlottenlund, Denmark

Submitted: July 12, 2019; Accepted: January 31, 2020
Proofs received from author(s): March 2, 2020